Application of the stopped flow technique to the TiO2-heterogeneous photocatalysis of hexavalent chromium in aqueous suspensions. Comparison with O2 and H2O2 as electron acceptors

Journal:	*Langmuir*
Manuscript ID:	la-2015-005744.R1
Manuscript Type:	Article
Date Submitted by the Author:	06-Apr-2015
Complete List of Authors:	Meichtry, Jorge; Comisión Nacional de Energía Atómica, Gerencia Química Dillert, Ralf; Universitaet Hannover, Institut für Technische ChemieCallinstraße 3 Bahnemann, Detlef; Universitaet Hannover, Institut für Technische ChemieCallinstraße 3 Litter, Marta; Comisión Nacional de Energía Atómica, Gerencia Química

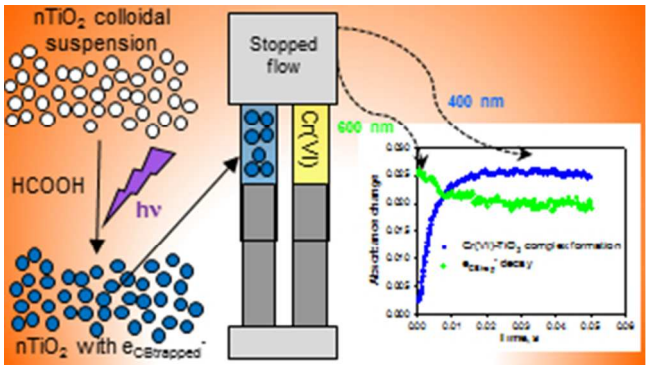

84x47mm (96 x 96 DPI)

Application of the stopped flow technique to the TiO_2-heterogeneous photocatalysis of hexavalent chromium in aqueous suspensions. Comparison with O_2 and H_2O_2 as electron acceptors

Jorge M. Meichtry[#,‡], Ralf Dillert[♠], Detlef W. Bahnemann[♠], Marta I. Litter[#,‡,♦]*

[#] Gerencia Química, Comisión Nacional de Energía Atómica, Av. Gral. Paz 1499, 1650 San Martín, Prov. de Buenos Aires, Argentina

[‡] Consejo Nacional de Investigaciones Científicas y Técnicas (CONICET), Av. Rivadavia 1917, 1033 Ciudad Autónoma de Buenos Aires, Argentina

[♠] Institut für Technische Chemie, Leibniz Universität Hannover, Callinstrasse 3, D-30167 Hannover, Germany

[♦] Instituto de Investigación e Ingeniería Ambiental, Universidad Nacional de General San Martín, Campus Miguelete, Av. 25 de Mayo y Francia, 1650 San Martín, Prov. de Buenos Aires, Argentina

ABSTRACT: The dynamics of the transfer of electrons stored in TiO_2 nanoparticles to Cr(VI) in aqueous solution have been investigated using the stopped flow technique. TiO_2 nanoparticles were previously irradiated under UV light in the presence of formic acid, and trapped electrons (e_{trap}^-) were made to react with Cr(VI) as acceptor species;

other common acceptor species such as O_2 and H_2O_2 were also tested. The temporal evolution of the amount of trapped electrons was followed by the decrease of the absorbance at 600 nm, and the kinetics of the electron transfer reaction was modeled. Additionally, the rate of formation of the surface complex between Cr(VI) and TiO_2 was determined with the stopped flow technique by following the evolution of the absorbance at 400 nm of suspensions of non-irradiated TiO_2 nanoparticles and Cr(VI) at different concentrations. An approximately quadratic relationship was observed between the maximum absorbance of the surface complex and the concentration of Cr(VI), suggesting that Cr(VI) adsorbs onto the TiO_2 surface as dichromate. The kinetic analyses indicate that the electron transfer from TiO_2 to Cr(VI) does not require the previous formation of the Cr(VI)-TiO_2 surface complex, at least the complex detected here through the stopped flow experiments. When previously irradiated TiO_2 was used to follow the evolution of the Cr(VI)-TiO_2 complex, an inhibition of the formation of the complex was observed, which can be related with the TiO_2 deactivation caused by Cr(III) deposition.

INTRODUCTION

TiO_2 heterogeneous photocatalysis is one of the Advanced Oxidation (Reduction) Technologies of the foremost interest due to its possible applications for the treatment of pollutants. The basic mechanism taking part in the process is well known, i.e., band gap excitation of semiconducting TiO_2 particles promotes the formation of electron and

hole pairs, with further redox reactions with species present at the interface. However, some mechanistic details of photocatalytic reactions still remain not completely elucidated.

The stopped flow spectrophotometric technique has been extensively used in kinetic studies of several chemical reactions due to its simplicity and short analysis time,[1] being ideal to follow reactions with lifetimes between 0.001 and some seconds. The dynamics of the transfer of electrons, previously generated in optically transparent TiO_2 nanoparticles by UV-A irradiation in the presence of a hole scavenger, to several chemical species can be studied by stopped flow.

In a previous short note, the dynamics of the transfer of electrons stored in TiO_2 to oxidants such as O_2 and H_2O_2 has been studied, and the reduction kinetics was followed by the temporal decay of the transient absorbance of the stored electrons at 600 nm.[2] In a further paper,[3] the stopped flow study has been extended to other chemical species such as NO_3^-, Cu(II), Zn(II) and Mn(II).

In the present paper, new insights on the electron transfer reaction from TiO_2 to Cr(VI), as well as to other model acceptors such as O_2 and H_2O_2, using stopped flow experiments, are presented.

EXPERIMENTAL SECTION

Materials. All chemicals were of the highest purity and were used as received: $TiCl_4$, $K_2Cr_2O_7$ and H_2O_2 (30%) were Sigma-Aldrich; formic acid (HCOOH) was

Merck. For pH adjustments, 1 M HCl (Merck) was used. All solutions were prepared with deionized water from a Sartorius Arium 611 apparatus (resistivity = 18.2 Ω cm).

Preparation of TiO_2 nanoparticles. The transparent TiO_2 nanoparticles (2-3 nm particle size) were prepared by following the method reported in Ref.[2] Briefly, a 3.5 mL solution of $TiCl_4$, prechilled to −20 °C, was added slowly to 900 mL of deionized water at 1 °C under vigorous magnetic stirring. After continuous stirring for 1 h, the resulting colloidal suspension was dialyzed against deionized water using a double dialysis membrane until a final pH between 2 and 3. The solution was kept at 5 °C for around 12 h under stirring, and the solvent was removed using a rotatory evaporator at 20-25 mbar and 27-30 °C. Off-white shining crystals were obtained, which were resuspended in pure water to obtain perfectly transparent colloidal TiO_2 suspensions with a final $[TiO_2]$ = 6 g L^{-1}. Hereinafter, these nanoparticles will be called $nTiO_2$.

Storing of electrons on TiO_2 nanoparticles. For the loading of $nTiO_2$, a glass cell (51 mL), provided with a sealed silicone cap, was used. The corresponding amount of TiO_2 suspension was mixed with water or with a HCOOH solution until a final suspension with $[TiO_2]$ = 3 g L^{-1} at pH 2 (HCl) was obtained; when used, final [HCOOH] was 40 mM. After N_2 bubbling for 30 min (at 0.5 L min^{-1}) to ensure dissolved O_2 removal (O_2 concentration ≤ 0.1 mg L^{-1}, the detection limit of the trioximaticEO 200 electrode used for O_2 control, see below), the suspension was irradiated with a high-pressure Hg-lamp (OSRAM HBO-500W), equipped with a quartz water filter to avoid IR radiation. The UV-A light intensity was 2.6×10^{-3} J cm^{-2} s^{-1}, measured with a UV radiometer LTLutron UVA-365.

Stopped flow experiments. The experiments were performed using an SX.18MV-R Rapid Mixing Spectrophotometer (Applied Photophysics), with a 2 mm optical path cell. The dead time of the equipment was ~3 ms, the residence time in the mixing cell was ~4 ms, with a receptor syringe volume of 500 μL and an injection syringe volume of 1000 μL. The detection light was obtained from a Spectra Kinetic Monochromator, operative between 200 and 700 nm, and using a 100 W tungsten incandescent lamp as light source.

In a typical experiment, a sample of a 3 g L^{-1} $nTiO_2$ suspension loaded with electrons was taken from the irradiation cell by penetrating the silicone cap with a needle attached to a dispensable syringe; then, the needle was removed and the suspension was carefully filled into one of the stopped flow syringes, and an aqueous solution containing the electron acceptor (Cr(VI), H_2O_2 or O_2) was filled into the other syringe. In the experiments without O_2, N_2 was bubbled into the solution containing the reactants for at least 15 min at 0.5 L min^{-1} ($[O_2] \leq 0.1$ mg L^{-1}), while in the experiments with O_2, the solution was left open to the air under magnetic stirring for at least 30 min. The solutions were injected into a mixing chamber (1:1 v/v), and the resulting reactant mixture was introduced into the optical cell where the temporal change of absorbance was measured. The reported concentration of reactants corresponds to the concentration in the injection syringe, the concentration in the detection cell being half this value. The decay of the absorbance of the trapped TiO_2 electrons (e_{trap}^-) at 600 nm or the build-up of the absorption signal of the Cr(VI)-TiO_2 complex at 400 nm were followed. For a

better comparison between the different runs, the absorption signals were always set to the same initial absorbance.

All stopped flow determinations were performed by triplicate and results averaged. The experimental error for the averaged experiments was always ≤ 5%, as calculated by standard deviation among the replicates. The fitting of the experimental points was performed with Origin 8.0 software, with reduced Chi-Sqr as iteration ending criterion.

Analytical methods. All UV-Vis spectra (200-800 nm) were recorded employing a Varian Cary 100 Scan UV-Vis system in a quartz cell of 1 cm optical path.

The concentration of dissolved oxygen in water was determined using a Microprocessor Oximeteroxi 2000 in combination with a TrioximaticEO 200 electrode.

RESULTS AND DISCUSSION

Storing of electrons on TiO_2 nanoparticles. The UV-A irradiation of a system containing nTiO_2 (3 g L^{-1}) and 40 mM HCOOH as hole scavenger in the absence of O_2 resulted in the formation of a transparent blue suspension, the color indicating the generation of the stored electrons (e_{trap}^-) in the nTiO_2 particles. The blue color is attributed to the formation of Ti(III) species, according to the following processes:

$$TiO_2 \rightarrow TiO_2 (e_{CB}^- + h_{VB}^+) \quad (1)$$

$$e_{CB}^- + TiO_2 \rightarrow e^-(Ti(III)) \quad (2)$$

where e^-(Ti(III)) ≡ e_{trap}^-. The spectrum of the irradiated $nTiO_2$ showed a broad absorption band from 510 to 700 nm with an absorbance maximum at 600 nm, in agreement with previous papers.[2-4] Generally, irradiation was performed for 24 h, to allow attaining the maximum of absorbance. In contrast with previous works where methanol was used as hole scavenger,[2,3] HCOOH was chosen in this paper because it is a better electron donor[5] and because the only reaction product is CO_2.[6,7] The h_{VB}^+ generated in $nTiO_2$ or the hydroxyl radicals formed by attack of holes to adsorbed water or surface hydroxyls (Eqs. (4) and (5)) are able to oxidize HCOOH, generating the very reducing $CO_2^{\bullet-}$ species ($E^0(CO_2/CO_2^{\bullet-}) \approx -2.0$ V),[8] which injects electrons into the TiO_2 CB:[9]

$$HCOOH + h_{VB}^+ \rightarrow CO_2^{\bullet-} + 2\,H^+ \quad (3)$$

$$H_2O_{ads} + h_{VB}^+ \rightarrow HO^\bullet + H^+ \quad (4)$$

$$HO_{surf}^- + h_{VB}^+ \rightarrow HO^\bullet \quad (5)$$

$$HCOOH + HO^\bullet \rightarrow CO_2^{\bullet-} + H_3O^+ \quad (6)$$

$$CO_2^{\bullet-} + TiO_2 \rightarrow e_{CB}^- + CO_2 \quad (7)$$

According to eqs. (1)-(7), the amount of consumed HCOOH should be equal to half the amount of [e_{trap}^-]; therefore, HCOOH was still present after [e_{trap}^-] reaches the maximum concentration.

To calculate the number of electrons per TiO_2 particle, the initial concentration of e_{trap}^- was determined using the value of the molar absorption coefficient, $\varepsilon_{600\ nm}$ = 600

M^{-1} cm^{-1}, reported previously and obtained through titration with benzoquinone,[3] and the absorbance of the difference spectrum at 600 nm (A = 0.32, Figure 1); from this, $[e_{trap}^-]$ = 0.53 mM (32×10^{19} electrons L^{-1}). Assuming that the TiO_2 nanoparticles have a spherical shape with a 3 nm diameter,[2] the volume of one TiO_2 particle is 1.41×10^{-20} cm^3. Considering the mass density of anatase, 3.894 g cm^{-3},[10] the average weight of one TiO_2 nanoparticle is 5.43×10^{-20} g. For $[TiO_2]$ = 3 g L^{-1}, the number of TiO_2 particles is then 5.53×10^{19} particles L^{-1}, corresponding to an average of about 5-6 electrons per TiO_2 particle.

Experiments with O_2. Water saturated with O_2 ($[O_2]$ = 0.27 mM, i.e. 0.135 mM in the stopped flow detection cell) was used as a probe of reaction with e_{trap}^-, i.e., the decay of these electrons. For the reaction of the electrons with oxygen, the following reaction takes place:[2,3,11]

$$O_2 + e_{trap}^- + H^+ \rightarrow HO_2^\bullet \quad (8)$$

$$HO_2^\bullet + e_{trap}^- + H^+ \rightarrow H_2O_2 \quad (9)$$

As it will be indicated later, H_2O_2 is transformed also by e_{trap}^-.[2,3,11]

Figure 1 describes the transformation of the spectrum of the initial $nTiO_2$ (black curve) after 120 min of UV irradiation in the presence of 40 mM HCOOH under N_2 (red curve). The green curve indicates the decay of electrons produced after exposure of the activated $nTiO_2$ suspension to O_2 in the absence of other acceptors and due to reactions (8) and (9). The black and green curves should be identical and their difference can be

attributed to some feature inherent to the nanoparticles, e.g., aggregation by an increase of the amount of surface hydroxyl groups under UV-A irradiation.[12] The blue curve, obtained by the difference of the red and green curves, corresponds to the absorbance of trapped electrons (e_{trap}^-). Small differences were found in the spectra of the irradiated $nTiO_2$ in different runs (cf. red line in Figure 1 and black line in Figure 4), most probably due to small differences in the temperature of the suspension during irradiation.

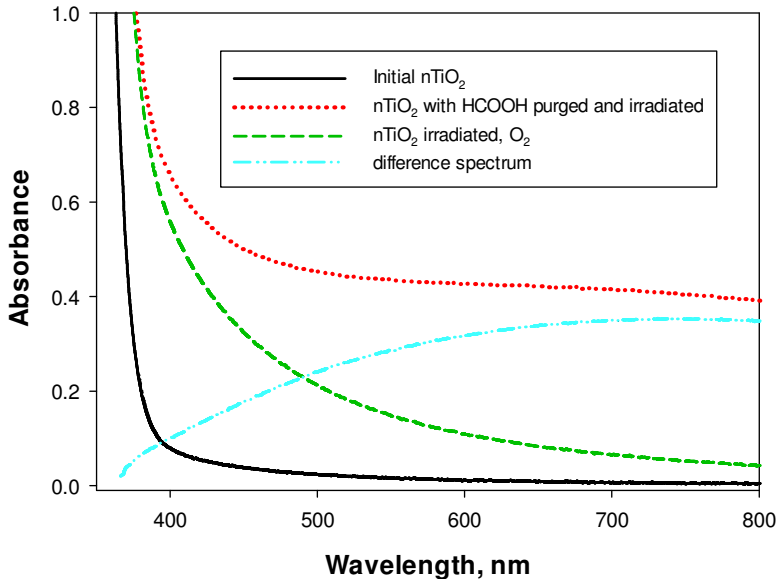

Figure 1. Spectra of initial $nTiO_2$ suspension (3 g L^{-1}, solid black line), after 120 min irradiation in the presence of 40 mM HCOOH at pH 2 under N_2 bubbling (red dotted line), and after reaction with O_2 (green dashed line). The blue dotted-dashed curve is the difference spectrum (difference of red and green curves).

Experiments with H_2O_2. Figure 2 shows the temporal profiles of the transient absorption signals observed upon mixing suspensions of TiO_2 with stored electrons ($[e_{trap}^-]$ = 0.53 mM) at pH 2 with aqueous solutions containing $[O_2]$ = 0.27 mM and different H_2O_2 concentrations ($0 \leq [H_2O_2] \leq 5$ mM), respectively. Additionally, water saturated with N_2 was employed to obtain a reference signal in the absence of any deliberately added electron acceptor, which enables estimating the decay of the absorbance of e_{trap}^- due to the unintentional entrance of small amounts of O_2 to the system. Experimental runs having a duration of 1 s (Figure 2a) and of 0.1 s (Figure 2b) are shown.

From this Figure, it becomes obvious that the absorbance of e_{trap}^- is decreasing in all runs. This also applies to experiments in which no electron acceptor was added (N_2-containing solution) indicating that O_2 is slowly diffusing from the surrounding environment into the detection cell. The drastic decrease of the signal of e_{trap}^- is observed after reaction with H_2O_2, due to the following reactions:[2,3,11]

$$H_2O_2 + e_{trap}^- + H^+ \rightarrow H_2O + HO^\bullet \quad (10)$$

$$HO^\bullet + e_{trap}^- + H^+ \rightarrow H_2O \quad (11)$$

According to Eqs. (10) and (11), the stoichiometry for complete H_2O_2 reduction is H_2O_2/e_{trap}^- = 1:2. Given that $[e_{trap}^-]$ = 0.53 mM for the experiments shown in Figure 2, at $[H_2O_2]$ = 0.1 mM incomplete e_{trap}^- consumption should be obtained. Assuming that

reaction (11) is faster than (10), this last reaction should be the rate-controlling step for H_2O_2 reduction.

The runs at $[H_2O_2] \geq 1$ mM can be more clearly appreciated in Figure 2(b), as the e_{trap}^- decay is too fast for the 1 s timescale. At $[H_2O_2] = 1$ mM, an almost complete e_{trap}^- decay is obtained within 0.1 s, as can be clearly observed in Figure 2(b), while for $[H_2O_2] = 10$ mM a smaller decay is appreciated, most probably due to a very fast e_{trap}^- decay even for the 0.1 s timescale, as will be discussed later.

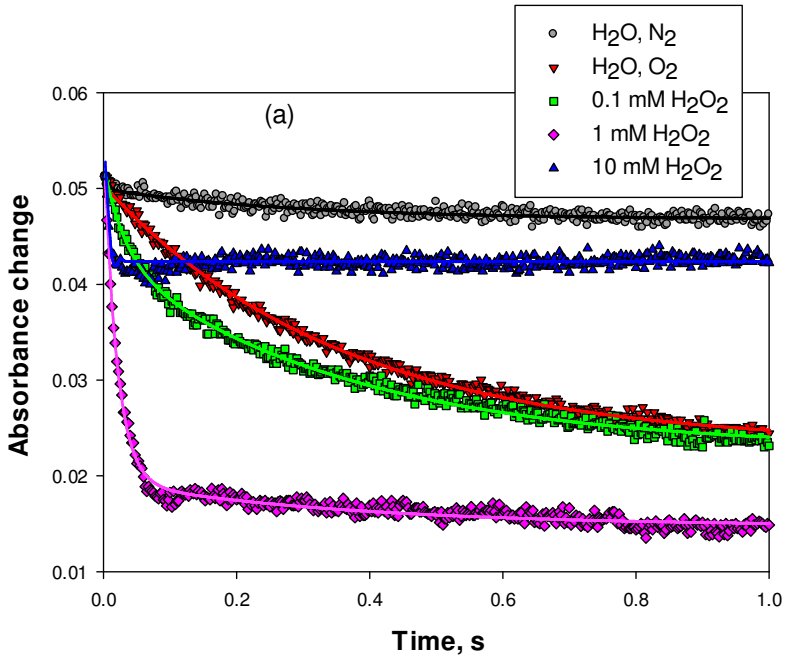

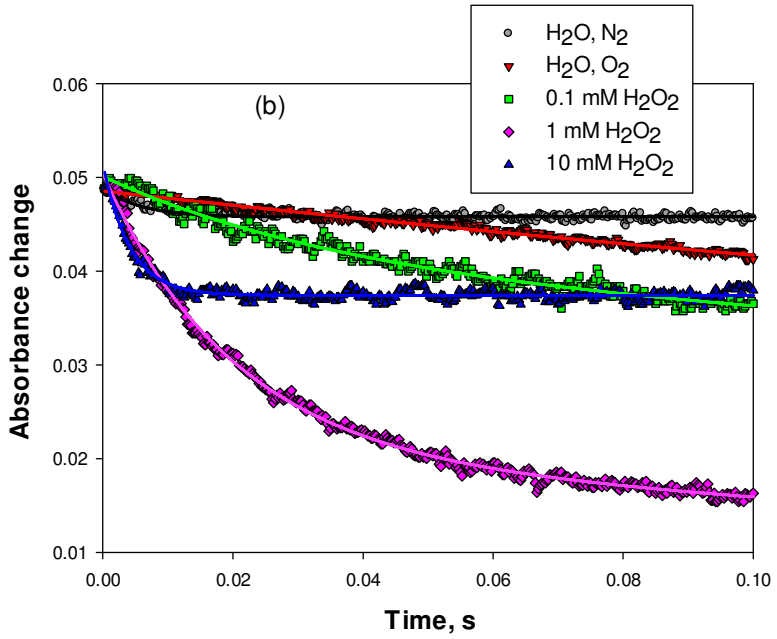

Figure 2. Time profile of the decay of the e_{trap}^- absorbance at 600 nm ($[e_{trap}^-]$ = 0.53 mM) upon mixing an $nTiO_2$ suspension (3 g L^{-1}) with an O_2 saturated aqueous solution ($[O_2]$ = 0.27 mM) at pH 2 and increasing H_2O_2 concentrations (0.1 (green squares), 1 (pink diamonds) and 10 mM (blue up-triangles)). Solid lines show the monoexponential fittings of experimental points for H_2O saturated with N_2 (gray circles), H_2O saturated with O_2 (red down-triangles) and 10 mM H_2O_2 to Eq. (16) and biexponential fittings for 0.1 and 1 mM H_2O_2 to Eq. (17). a) 1 s Run; b) 0.1 s run.

Experiments with Cr(VI). Figure 3 shows the temporal profiles of the transient absorption signals observed upon mixing suspensions of TiO_2 with stored electrons ($[e_{trap}^-]$ = 0.53 mM) at pH 2 with Cr(VI) solutions at different concentrations in the absence of O_2; the reaction with O_2 of Figure 2 is included for comparison.

The photocatalytic reduction of Cr(VI) in water has been widely reported in the literature.[13,14] This photocatalytic system, where Cr(III) is the final stable product, is unique: Cr(VI) is the only metal species whose reductive TiO_2 photocatalytic removal is not influenced by the presence of oxygen, at least at acid pH, in contrast with most metals; this has been explained by the fast capture of electrons caused by a very strong association between Cr(VI) and TiO_2 through the formation of a charge-transfer complex.[15]

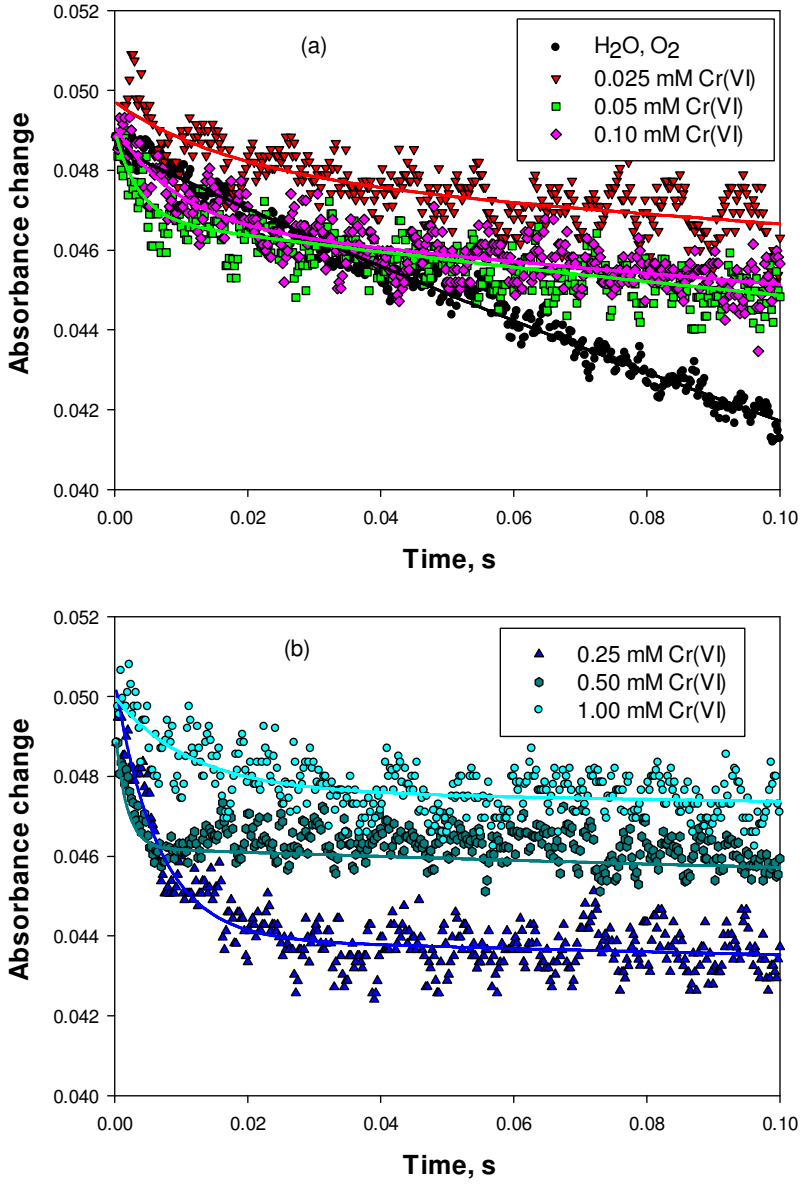

Figure 3. Time profile of the decay of the e_{trap}^- absorbance at 600 nm ($[e_{trap}^-]$ = 0.53 mM) upon mixing with Cr(VI) solutions at different concentrations (0.025 (red down-triangles), 0.05 (green squares), 0.10 (pink diamonds), 0.25 (blue up-triangles), 0.50 (green hexagons), 1 (turquoise circles) mM) in the absence of O_2 at pH 2. Solid lines show the monoexponential fittings of the experimental points for H_2O saturated with O_2 (black circles) to Eq. (16), and biexponential fittings of the experimental points for Cr(VI) to Eq. (17). a) 0.1 s Run for 0.025 to 0.1 mM; b) 0.1 s run for 0.25 to 1 mM.

In this case, the decay of e_{trap}^- absorbance at 600 nm seen through the stopped flow experiments is due to the following reactions:

$$Cr(VI) + e_{trap}^- \rightarrow Cr(V) \quad (12)$$

$$Cr(V) + e_{trap}^- \rightarrow Cr(IV) \quad (13)$$

$$Cr(IV) + e_{trap}^- \rightarrow Cr(III) \quad (14)$$

Given that Cr(V) and Cr(IV) are very unstable and reactive species, with one electron reduction potentials much more positive than that of Cr(VI),[16] it can be proposed that the rate controlling step is Eq. (12). Figure 3 shows that for all Cr(VI) concentrations, the decay of e_{trap}^- absorbance was much smaller than that observed for the reaction with O_2; also, in stopped flow runs lasting 10 s (not shown), no significant change of absorbance (i.e., $\geq$ 0.015) was observed for any Cr(VI) value. Although this can be considered as an indication that the reaction between e_{trap}^- and Cr(VI) is almost

negligible, it is more probably that this could be due to: 1) a very fast reaction between e_{trap}^- and Cr(VI), by which only the final decay of the e_{trap}^- can be observed with the stopped flow technique, and/or 2) the absorbance at 600 nm includes those of intermediate and final Cr(VI) reduction species, avoiding the detection of small absorbance changes. Taking into account that Cr(V) and Cr(IV) are very unstable species with short lifetimes and that the ε_{600nm} value for Cr(III) is around 10 M^{-1} cm^{-1},[17] the contribution of reduced chromium species to the signal at 600 nm can be considered very low. This indicates that the reaction between e_{trap}^- and Cr(VI) is too fast for the temporal resolution of the stopped flow technique (0.001 s).

Figure 4 shows the spectra of samples collected in the stopping syringe of the apparatus, i.e., at the end of the stopped flow runs for the experiments without Cr(VI) and with 0.1, 0.25 and 1 mM Cr(VI).

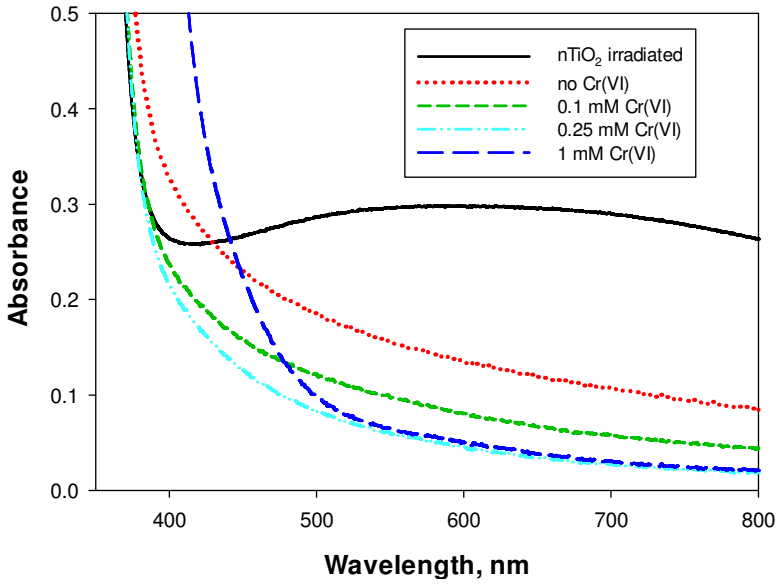

Figure 4. Spectra of the samples obtained in the stopping syringe after stopped flow experiments of irradiated $nTiO_2$ with Cr(VI) solutions at different concentrations. Conditions of Figure 3. Initial $nTiO_2$ suspension (3 g L^{-1}, solid black line), [Cr(VI)] = 0 (red dotted line), [Cr(VI)] = 0.1 mM (green dashed line), [Cr(VI)] = 0.25 mM (turquoise dotted-dashed line), [Cr(VI)] = 1 mM (blue dashed line).

The difference in the absorbance at 600 nm between the spectra without Cr(VI) and at 0.25 mM or 1 mM Cr(VI) (0.090) can be considered the full decay of the e_{trap}^-, while the difference between the spectra without Cr(VI) and at 0.1 mM Cr(VI) (0.055) represents 61% of the full decay. Consequently, it can be calculated that 0.165 mM Cr(VI) is the minimum amount of Cr(VI) required to react completely (100%) with e_{trap}^-. Using the stoichiometry proposed in Eq. (15), an initial value of 0.495 mM can be calculated for $[e_{trap}^-]$, very similar to the value of 0.53 mM determined using the absorption at 600 nm of the irradiated $nTiO_2$ (vide supra). This indicates that the stoichiometry proposed in Eq. (15) is accurate, and that only e_{trap}^- are involved in Cr(VI) reduction to Cr(III).

$$Cr(VI) + 3\ e_{trap}^- \rightarrow Cr(III) \qquad (15)$$

This observation is very significant, as it should be considered that formic acid, remaining from the irradiation procedure for accumulating e_{trap}^-, is still present in the $nTiO_2$ suspension used in the stopped-flow measurements. According to Eqs. (12)-(14),

Cr(V) and Cr(IV) are formed in the system, and they can react with formic acid very rapidly and faster than Cr(VI).[18-20] However, given that the consumption of e_{trap}^- by Cr(VI) closely follows the stoichiometry of Eq. (15), the reaction of Cr(V) and/or Cr(IV) with HCOOH is much slower than that with e_{trap}^-; otherwise, less than 3 e_{trap}^- would be required to reduce Cr(VI) and the value of $[e_{trap}^-]$ calculated from the spectra of Figure 4 would be higher.

Kinetic calculations for the electron transfer reactions. The experimental points of Figures 2 and 3 could be adjusted to pseudo first order decays (solid lines), either mono- or biexponential, according to the following expressions:

$$\Delta A = \Delta A_0 + \Delta A_1 \times e^{-k_1 t} \quad (16)$$

$$\Delta A = \Delta A_0 + \Delta A_1 \times e^{-k_1 t} + \Delta A_2 \times e^{-k_2 t} \quad (17)$$

where ΔA_0 is the constant absorbance at infinite time, ΔA_1 and ΔA_2 are the decays of the absorbance due to two different first order reaction pathways, and k_1 and k_2 are the kinetic constants of each process. According to Eq. (17), the decay would take place through a mechanism involving two simultaneous process, 1 and 2, from which process 1 will be assumed to be the fastest one. The kinetic parameters are shown in Table 1. For the fittings, the value of k_1 obtained for O_2, i.e. 2.8 s^{-1}, was used to adjust the experimental points of H_2O_2 and Cr(VI), while the other parameters were allowed to vary freely.

Table 1. Kinetic parameters obtained from the fitting of the experimental points of Figures 2 and 3 with Eqs. (16) and (17).

Acceptor/mM	ΔA_0	ΔA_1	k_1, s^{-1}	ΔA_2	k_2, s^{-1}	R^2
H_2O, N_2	0.0470 ± 0.0001	0.0037 ± 0.0001	2.8 ± 0.1	---	---	0.776
O_2/0.27	0.0231 ± 0.0001	0.0272 ± 0.0001	2.8 ± 0.1	---	---	0.995
O_2/0.27 (10 s run)	0.0136 ± 0.0001	0.0272 ± 0.0001	2.8 ± 0.1	0.0107 ± 0.0001	0.44 ± 0.01	0.985
H_2O_2/0.1	0.0228 ± 0.0001	0.0095 ± 0.0001	31 ± 2	0.02 ± 0.0002	2.8	0.992
H_2O_2/1	0.0148 ± 0.0001	0.036 ± 0.0004	51 ± 1	0.0047± 0.0002	2.8	0.996
H_2O_2/10 (0.1 s run)	0.0374 ± 0.0004	0.0140 ± 0.0003	240 ± 8	0 ± 0.0004	2.8	0.925
Cr(VI)/0.025	0.043 ± 0.001	0.0017 ± 0.0003	58 ± 20	0.005 ± 0.002	2.8	0.653
Cr(VI)/0.05	0.0450 ± 0.0004	0.0022 ± 0.0002	282 ± 56	0.0079 ± 0.0004	2.8	0.703
Cr(VI)/0.10	0.0400 ± 0.0004	0.0024 ± 0.0002	108 ± 17	0.0064 ± 0.0007	2.8	0.753

Cr(VI)/0.25	0.0422 ± 0.0004	0.0065 ± 0.0002	167 ± 13	0.0017 ± 0.0005	2.8	0.820
Cr(VI)/0.50	0.0450 ± 0.0003	0.0031 ± 0.0003	575 ± 93	0.0020 ± 0.0003	2.8	0.415
Cr(VI)/1.00	0.0465 ± 0.0003	0.0023 ± 0.0003	89 ± 17	0.0012 ± 0.0009	2.8	0.504

Good correlation coefficients ($R^2 \geq 0.9$) could be obtained for the experiments with O_2 and H_2O_2, where a significant absorbance change (≥ 0.027) within the time of an experimental run could be measured. Although the R^2 values for the Cr(VI) runs may reflect that Eq. (17) is not a good model for this system, a random distribution of the residuals around the adjusted value was obtained from the corresponding fittings, indicating the accuracy of the biexponential regime. The low R^2 may be attributed, instead, to the small decay of e_{trap}^- (i.e., the sum of $\Delta A_1 + \Delta A_2$), which was in the same order of magnitude as the detection limit (absorbance change = 0.001). The values obtained for ΔA_2 in the experiments with [Cr(VI)] = 0.1 mM are similar to the values obtained for ΔA_1 in the experiment with H_2O/N_2, reinforcing the assumption that, in these experiments, the e_{trap}^- decay related with ΔA_2 is due to the oxygen that enter into the system during the stopped flow run (as already assumed by fixing the value of k_2 equal to 2.8 s^{-1}).

Contrarily to that observed by Mohamed et al.,[2] a monoexponential decay adjusted the experimental points of the reaction with O_2 in Figure 2, but this is only due to the different timescale used by the authors (20 s) and by us (0.1 and 1 s), as rather long measurement times (around 10 s) are required to appreciate the biexponential behavior. Actually, in one run done up to 10 s (not shown), a double exponential decay was observed. A simple calculation using Eq. (18) with the k_1 value of Table 1 and the oxygen concentration in the detection cell, i.e. $[O_2] = 0.135$ mM:

$$k = k^{obs} \times [\text{electron acceptor}] \quad (18)$$

allows to calculate a second order constant for the reaction with O_2 of 2.1×10^4 M^{-1} s^{-1}, in good agreement with that reported in Ref.[2] ($k_I^{obs} = 2.0 \times 10^4$ M^{-1} s^{-1}). From the value of k_2 calculated for the 10 s run with O_2, i.e., 0.44 s^{-1}, a second order constant of 3.2×10^3 M^{-1} s^{-1} can be obtained, quite similar to the value obtained in the same Ref.[2] for k_2^{obs} (5.6×10^3 M^{-1} s^{-1}).

For the other acceptors, i.e., H_2O_2 and Cr(VI), double exponential decays were observed in all cases, with the exception of $[H_2O_2]$ = 10 mM. For H_2O_2, the value of k_1 increases as the concentration increases, indicating a faster reaction; also, the contribution of the fast process to the e_{trap}^- decay increases when $[H_2O_2]$ increases from 0.1 to 1 mM, as reflected by the increase in ΔA_1; the smaller value obtained at 10 mM H_2O_2 compared with that at 1 mM H_2O_2 (0.014 and 0.036, respectively) should be related with the very high k_1 (240 s^{-1}), which indicates that a significant e_{trap}^- decay took place during the dead time of the run. Correspondingly, the e_{trap}^- decay by the slow process (ΔA_2) decreases. As O_2 was present in the runs with H_2O_2, it can be suggested that the fast process is linked with the reaction of e_{trap}^- with H_2O_2 and the slow one to their reaction with O_2. The dependence of k_1 with $[H_2O_2]$ is less than linear, indicating that the process is not a first order one. For 1 mM H_2O_2, a second order rate constant of $k_I^{obs} = 4.8 \times 10^5$ M^{-1} s^{-1} can be calculated with Eq. (18), very similar to the value obtained in Ref.[2] ($k_I^{obs} = 2.7 \times 10^5$ M^{-1} s^{-1}).

For the experiments with Cr(VI), a significant decay attributable to reaction with e_{trap}^- was obtained only at [Cr(VI)] = 0.25 mM ($\Delta A_1 = 0.006$); using the value of k_1 = 167 s^{-1}, a second order rate constant of 1.34×10^6 M^{-1} s^{-1} can be calculated, i.e. 150 and

5 times higher than those obtained in this work for O_2 (k_I^{obs} = 2.1 × 10^4 M^{-1} s^{-1}) and H_2O_2 (k_I^{obs} = 4.8 × 10^5 M^{-1} s^{-1}), respectively. Again, the fast process is linked with the reaction of e_{trap}^- with Cr(VI), while the slow process can be related to the reaction with small amounts of O_2 entering the system when the stopped-flow is triggered; the contribution of this process to the decay of e_{trap}^- is always small ($\Delta A_2 \leq 0.008$), and is negligible at [Cr(VI)] ≥ 0.25 mM, i.e., when the full decay of e_{trap}^- can be attained (see Figure 4). This reinforces the assumption of all our previous works that Cr(VI) reacts very rapidly with electrons and that the presence of O_2 has no influence on the photocatalytic Cr(VI) reactions.[13-15]

Formation of the Cr(VI)-TiO_2 surface complex. Figure 4 shows that, after mixing irradiated nTiO_2 with 1 mM Cr(VI), not only a decrease in the absorbance at 600 nm, but also an increase around 400 nm can be observed; this increase can be related with the formation of the surface complex between Cr(VI) and TiO_2 already reported by our group, and detected by UV-Vis spectrophotometry.[15] Figure 5 clearly reveals the formation of this complex when the spectrum of a 3 g L^{-1} nTiO_2 suspension (not irradiated) containing 1 mM Cr(VI) at pH 2 is compared with the spectra of the separated components.

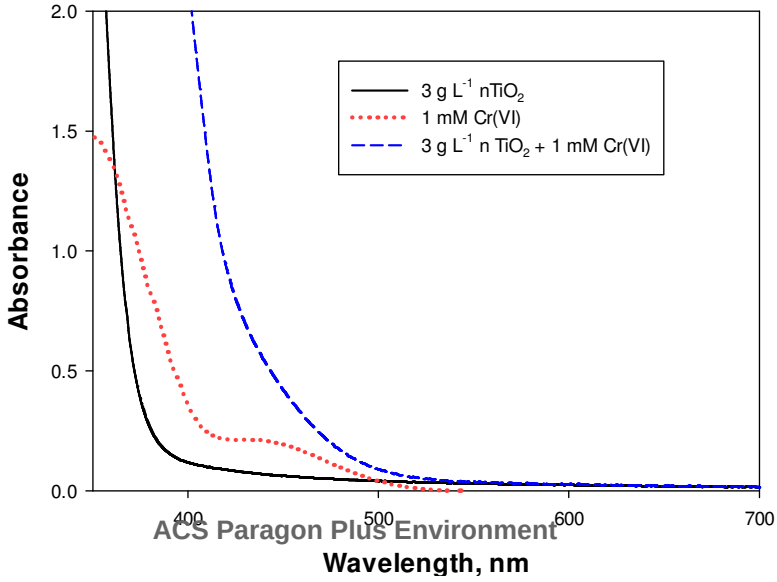

Figure 5. Spectra of a 3 g L^{-1} $nTiO_2$ suspension, an 1 mM Cr(VI) solution and a 3 g L^{-1} $nTiO_2$ suspension (not irradiated) with 1 mM Cr(VI) at pH 2.

The formation of the complex was followed by stopped flow at 400 nm, as indicated in Figure 6; this wavelength was chosen because it gave the best sensitivity for the determination, considering the absorbance of the complex (which increases steadily from 500 to the UV region, see Figure 5), the emission of the stopped flow lamp and the filter effect caused by $nTiO_2$ in the UV region. The formation of the complex between previously irradiated $nTiO_2$ and 1 mM Cr(VI) is also included.

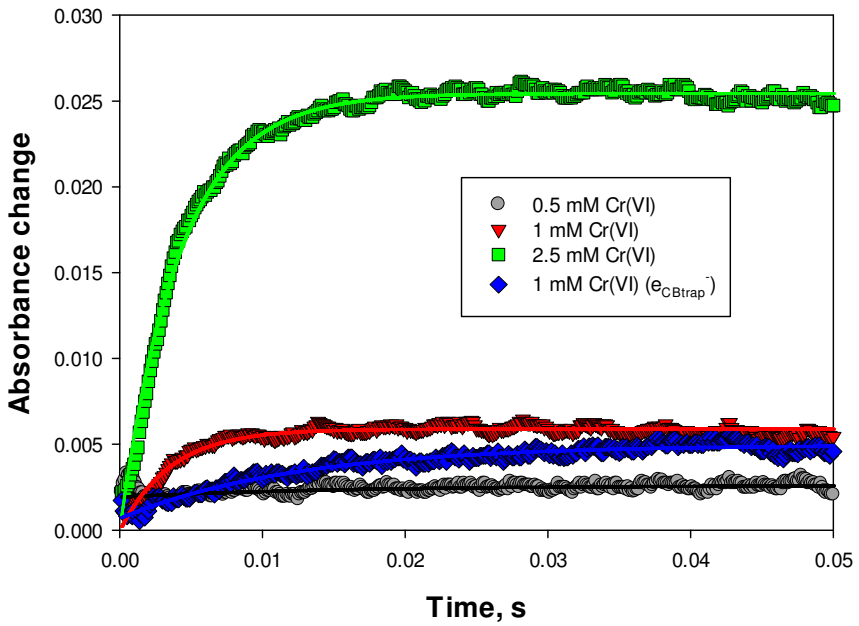

Figure 6. Temporal profile of the formation of the Cr(VI)-TiO_2 complex at different [Cr(VI)] with non-irradiated $nTiO_2$. A run with previously irradiated $nTiO_2$ and 1 mM Cr(VI) is included. Conditions: [$nTiO_2$] = 3 g L^{-1}; pH 2; measurement at λ = 400 nm. Solid lines show the monoexponential fittings of experimental points to Eq. (16).

The kinetics of the formation of the Cr(VI)-TiO_2 could be fitted to a pseudo first order behavior according to Eq. (16):

$$\Delta A = \Delta A_{max} (1\text{-}e^{-kt}) \quad (19)$$

where ΔA_{max} is the absorbance change at 400 nm due to the formation of the complex at infinite time and k' is the rate constant. The fitting parameters are indicated in Table 2. The kinetics could not be followed at [Cr(VI)] ≥ 10 mM because the increase of the ionic strength caused aggregation of the nTiO_2 particles and increase in light dispersion, turning the system unfitted for stopped flow measurements.

Table 2. Kinetic parameters obtained from the fitting of the experimental points of Figure 6 with Eq. (16)

[Cr(VI)], mM	ΔA_{max}	k', s^{-1}	R^2
0.5	0.001	63	0.410
1.0	0.006	282	0.900
1.0 (e_{trap}^-)	0.004	81	0.942
2.5	0.025	240	0.989

The R^2 values are reasonable in all cases, with the exception of 0.5 mM Cr(VI), where the very small change of absorbance avoided a good fitting. The k' value is not

constant, and depends strongly on [Cr(VI)], indicating that the formation of the complex occurs by a complicated mechanism that not follow a first order kinetics. For [Cr(VI)] = 5 mM the values deviated from the monoexponential behavior, suggesting a more complicated kinetics probably due to the formation of more than one type of surface complex. Actually, it has been previously reported that Cr(VI) can be adsorbed in different modes onto P25 TiO_2,[21], i.e., more than one surface complex would be possible between Cr(VI) and TiO_2.

When the formation of the complex is analyzed using a previously irradiated nTiO_2 suspension containing 1 mM Cr(VI), a decrease in the ΔA_{max} and k values can be appreciated compared with a similar same run with non-irradiated nanoparticles. This indicates that Cr(VI) reduction by e_{trap}^- inhibits the formation of the Cr(VI)-TiO_2 complex, which can be ascribed to Cr(III) deposition over the TiO_2 surface, as recently studied by our group;[22] this means that Cr(III) not only deactivates the photocatalyst surface by acting as an electron/hole recombination center,[22-24] but also by inhibiting the formation of the Cr(VI)-TiO_2 complex.

From the ΔA_{max} values for the experiments with non-irradiated n TiO_2^-, the following relationship has been obtained:

$$\Delta A_{max} = 0.0046 \times [Cr(VI)]^2 \text{ (mM)} \ (R^2 = 0.998) \quad (20)$$

The quadratic relationship between the concentration of the complex (ΔA_{max}) and [Cr(VI)] is in good agreement with results of Ref.,[21] which indicate that one of the

modes of Cr(VI) adsorption over TiO_2 implies Cr(VI) surface dimerization to dichromate.

The highest pseudo first order constant for the formation of the Cr(VI)-TiO_2 complex (282 s^{-1}) was obtained at [Cr(VI)] = 1 mM. From the second order rate constant calculated for the reaction between e_{trap}^- and Cr(VI), i.e. 1.34×10^6 M^{-1} s^{-1}, a pseudo first order constant of 670 s^{-1} can be calculated at the same Cr(VI) concentration. As the pseudo first order kinetic constant for the reaction of e_{trap}^- with Cr(VI) is more than twice that calculated for the complex formation under the same conditions (i.e. 282 s^{-1}), it can be postulated, as a very important result, that the electron transfer from TiO_2 to Cr(VI) does not require the previous formation of the Cr(VI)-TiO_2 surface complex, at least the one detected here by the stopped flow experiments.

CONCLUSIONS

The stopped flow technique allowed the calculation of kinetic parameters for electron transfer reactions to O_2, H_2O_2 and Cr(VI) from TiO_2 nanoparticles (previously irradiated under UV light in the presence of formic acid) and for the formation of the Cr(VI)-TiO_2 complex. Double exponential decays were observed in all cases with the exception of the cases of O_2 and the highest [H_2O_2] (10 mM), where a monoexponential decay was obtained. An approximately quadratic relationship was observed between A_{max} and [Cr(VI)], suggesting that Cr(VI) adsorbs onto TiO_2 in the form of dichromate. The inhibition observed in the formation of the Cr(VI)-TiO_2 complex when e_{CBtrap}^--

containing $nTiO_2$ is used, i.e., when Cr(VI) can be reduced to Cr(III), was related with the TiO_2 deactivation caused by Cr(III) deposition.

The stopped flow technique represents a very useful tool for these kinetic studies, which throw light to the fundamental pathways of photocatalytic reactions. This is the first time that this technique has been applied to the study of the Cr(VI) photocatalytic system and it allowed to confirm previously found features of the system, as the formation of the complex between Cr(VI) and TiO_2 and the lack of effect of O_2 in the reduction of the metal. Finally, it should be emphasized that the kinetic analyses indicate that the electron transfer from TiO_2 to Cr(VI) does not require the previous formation of the Cr(VI)-TiO_2 surface complex, at least the complex detected here through the stopped flow experiments.

ACKNOWLEDGEMENTS

This work was performed as part of Agencia Nacional de Promoción Científica y Tecnológica PICT-0463 and CONICET-DFG 183/13 projects. To Hanan Mohamed for help during the preparation of $nTiO_2$.

AUTHOR INFORMATION

Corresponding Author

*E-mail litter@cnea.gov.ar; marta.litter@gmail.com

Gerencia Química, Comisión Nacional de Energía Atómica, Av. Gral. Paz 1499, 1650 San Martín, Prov. de Buenos Aires, Argentina.

Notes

The authors declare no competing financial interest.

REFERENCES

(1) Beckwith P. M.; Crouch, S. R. An Automated Stopped-Flow Spectrophotometer with Digital Sequencing for Millisecond Analyses. *Anal. Chem.* **1972**, *44*, 221–227.

(2) Mohamed, H. H.; Dillert, R.; Bahnemann, D. W. Reaction Dynamics of the Transfer of Stored Electrons on TiO_2 Nanoparticles: A Stopped Flow Study. *J. Photochem. Photobiol. A*, **2011**, *217*, 271–274.

(3) Mohamed, H. H.; Mendive, C. B.; Dillert, R.; Bahnemann, D. W. Kinetic and Mechanistic Investigations of Multielectron Transfer Reactions Induced by Stored Electrons in TiO_2 Nanoparticles: A Stopped Flow Study. *J. Phys. Chem. A* **2011**, *115*, 2139–2147.

(4) Gao, R.; Safrany, A.; Rabani, J. Fundamental Reactions in TiO_2 Nanocrystallite Aqueous Solutions studied by Pulse Radiolysis. *Radiat. Phys. Chem.* **2002**, *65*, 599–609.

(5) Nguyen, V. N. H.; Amal, R.; Beydoun, D. Effect of Formate and Methanol on Photoreduction/Removal of Toxic Cadmium Ions Using TiO_2 Semiconductor as Photocatalyst. *Chem. Eng. Sci.* **2003**, *58*, 4429 – 4439.

(6) Serpone, N.; Martin, J.; Horikoshi, S.; Hidaka, H. Photocatalyzed Oxidation and Mineralization of C1–C5 Linear Aliphatic Acids in UV-irradiated Aqueous Titania Dispersions—Kinetics, Identification of Intermediates and Quantum Yields. *J. Photochem. Photobiol. A* **2005**, *169*, 235–251.

(7) Henderson, M. A. A Surface Science Perspective on TiO_2 Photocatalysis. *Surf. Sci. Reports* **2011**, *66*, 185–297.

(8) Wardman, P. J. Reduction Potentials of One-electron Couples Involving Free Radicals in Aqueous Solution. *J. Phys. Chem. Ref. Data* **1989**, *18*, 1637–1755.

(9) Perissinotti, L. L.; Brusa, M. A.; Grela, M. A. Yield of Carboxyl Anion Radicals in the Photocatalytic Degradation of Formate over TiO_2 Particles. *Langmuir* **2001**, *17*, 8422–8427.

(10) Burdett, J. K.; Hughbanks, T.; Miller, G. J.; Richardson Jr., J. W.; Smith, J. V. Structural-electronic Relationships in Inorganic Solids: Powder Neutron Diffraction Studies of the Rutile and Anatase Polymorphs of Titanium Dioxide at 15 and 295 K. *J. Am. Chem. Soc.* **1987**, *109*, 3639–3646.

(11) Gerischer, H.; Heller, A. The Role of Oxygen in Photooxidation of Organic Molecules on Semiconductor Particles. *J. Phys. Chem.*, **1991**, *95*, 5261–5267.

(12) Sun, J.; Guo, L. -H.; Zhang, H.; Zhao, L. UV Irradiation Induced Transformation of TiO_2 Nanoparticles in Water: Aggregation and Photoreactivity. *Environ. Sci. Technol.* **2014**, *48*, 11962–11968.

(13) Litter, M. I. Heterogeneous Photocatalysis. Transition Metal Ions in Photocatalytic Systems. *Appl. Catal. B* **1999**, *23*, 89–114.

(14) Litter, M. I. Mechanisms of Removal of Heavy Metals and Arsenic from Water by TiO_2-heterogeneous Photocatalysis. *Pure Appl. Chem.* **2014**, DOI: 10.1515/pac-2014-0710, January 2015.

(15) Di Iorio, Y.; San Román, E.; Litter, M. I.; Grela, M. A. Photoinduced Reactivity of Strongly Coupled TiO_2 Ligands under Visible Irradiation. An Examination of Alizarin Red @TiO_2 Nanoparticulate System. *J. Phys. Chem. C.* **2008**, *112*, 16532–16538.

(16) Niki, K. Chromium, Standard Potentials In Aqueous Solution, Editors: J. A. Bard, R. Parsons, J. Jordan, Taylor & Francis, New York, **1985**, 453–461.

(17) Protsenko, V. S.; Kityk, A. A.; Danilov, F. I. Electroreduction of Cr(III) Ions in Methanesulphonate Solution on Pb Electrode. *E-J. Chem.* **2011**, *8*, 1714–1719.

(18) Kemp, T. J.; Waters, W. A. The Mechanisms of Oxidation of Formaldehyde and Formic Acid by Ions of Chromium (VI), Vanadium (V) and Cobalt (III). *Proc. Royal Soc. A Math. Phys. Eng. Sci.* **1963**, *274*, 480–499.

(19) Krumpolc, M.; Rocek, J. Chromium(V) Oxidations of Organic Compounds. *Inorg. Chem.* **1985**, *24*, 617–621.

(20) Das, A. K. Kinetics and Mechanism of the Chromium(VI) Oxidation of Formic Acid in the Presence of Picolinic Acid and in the Presence and Absence of Surfactants. *Inorg. React. Mech.* **1999**, *1*, 161–168

(21) García Ródenas, L. A.; Weisz, A. D.; Magaz, G. E.; Blesa, M. A. Effect of Light on the Electrokinetic Behavior of TiO_2 Particles in Contact with Cr(VI) Aqueous Solutions. *J. Coll. Int. Sci.* **2000**, *230*, 181–185.

(22) Meichtry, J. M.; Colbeau-Justin, C.; Custo, G.; Litter, M. I. Preservation of the Photocatalytic Activity of TiO_2 by EDTA in the Reductive Transformation of Cr(VI). Studies by Time Resolved Microwave Conductivity. *Catal. Today* **2014**, *224*, 236–243.

(23) Herrmann, J. M. Detrimental Cationic Doping of Titania in Photocatalysis: why Chromium Cr^{3+}-Doping is a Catastrophe for Photocatalysis, both under UV- and Visible Irradiations. *New J. Chem.* **2012**, *36*, 883–890.

(24) Wang, N.; Xu, Y.; Zhu, L.; Shen, X.; Tang, H. Reconsideration to the deactivation of TiO_2 catalyst during simultaneous photocatalytic reduction of Cr(VI) and oxidation of salicylic acid. *J. Photochem. Photobiol. A* **2009**, *201*, 121–127.

Table of Contents Graphic

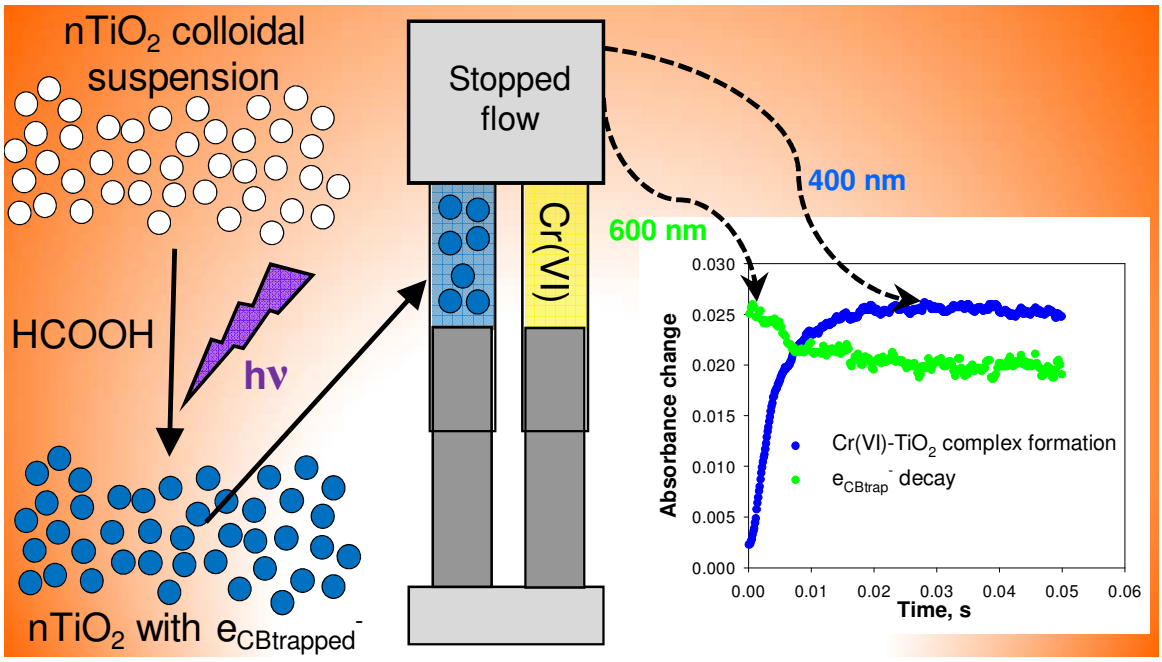

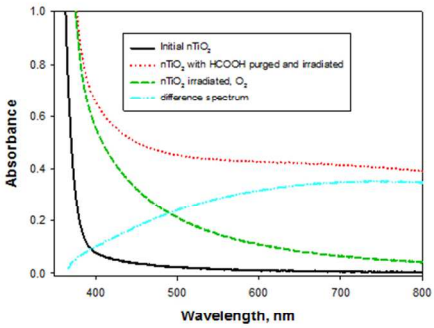

Figure 1. Spectra of initial nTiO2 suspension (3 g L−1), after 120 min irradiation in the presence of 40 mM HCOOH at pH 2 under N2 bubbling, and after reaction with O2. The blue curve is the difference spectrum (difference of red and green curves).
254x190mm (96 x 96 DPI)

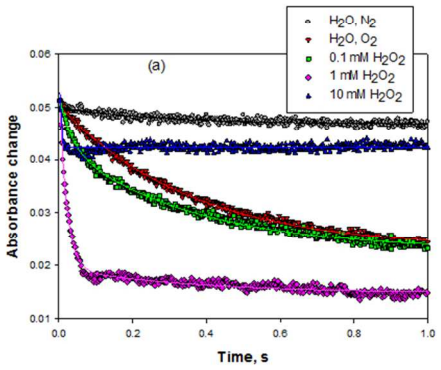

254x190mm (96 x 96 DPI)

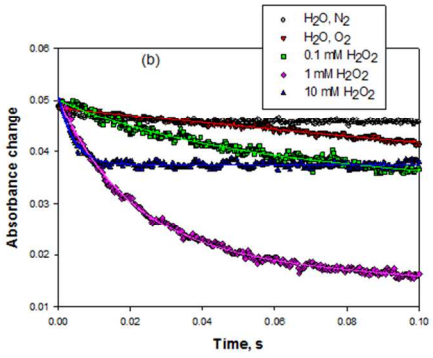

254x190mm (96 x 96 DPI)

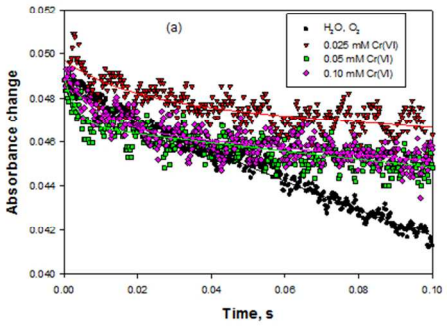

254x190mm (96 x 96 DPI)

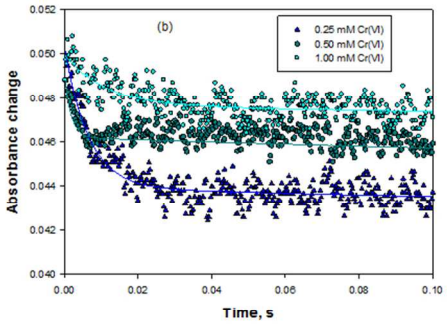

Figure 3. Time profile of the decay of the eCBtrap− absorbance at 600 nm ([eCBtrap−] = 0.53 mM) upon mixing with Cr(VI) solutions at different concentrations (0.025 to 1 mM) in the absence of O2 at pH 2. Solid lines show the monoexponential fittings of the experimental points for H2O saturated with O2 to Eq. (16), and biexponential fittings of the experimental points for Cr(VI) to Eq. (17). a) 0.1 s Run for 0.025 to 0.1 mM ; b) 0.1 s run for 0.25 to 1 mM.
254x190mm (96 x 96 DPI)

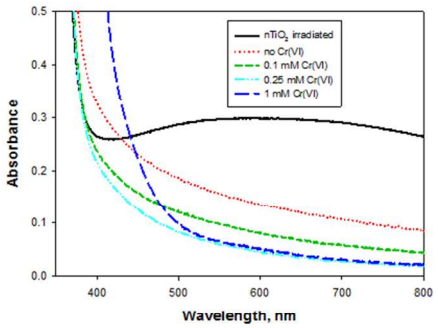

Figure 4. Spectra of the samples obtained in the stopping syringe after stopped flow experiments of irradiated nTiO2 with Cr(VI) solutions at different concentrations. Conditions of Figure 3.
254x190mm (96 x 96 DPI)

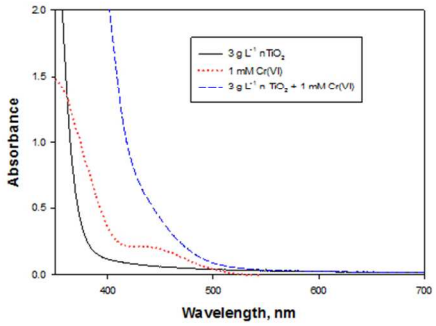

Figure 5. Spectra of a 3 g L−1 nTiO2 suspension, a 1 mM Cr(VI) solution and a 3 g L−1 nTiO2 suspension (not irradiated) with 1 mM Cr(VI) at pH 2.
254x190mm (96 x 96 DPI)

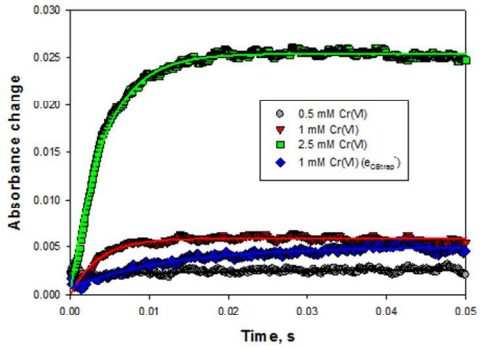

254x190mm (96 x 96 DPI)